JPE 17-2-21

https://doi.org/10.6113/JPE.2017.17.2.533
ISSN(Print): 1598-2092 / ISSN(Online): 2093-4718

A Novel Parameter-independent Fictive-axis Approach for the Voltage Oriented Control of Single-phase Inverters

Fernando Arturo Ramírez*, Marco A. Arjona†, and Concepcion Hernández*

*,†Dept. of Electrical and Electronic Engineering, Instituto Tecnológico de La Laguna, Torreon, Mexico

Abstract

This paper presents a novel Parameter-Independent Fictive-Axis (PIFA) approach for the Voltage-Oriented Control (VOC) algorithm used in grid-tied single-phase inverters. VOC is based on the transformation of the single-phase grid current into the synchronous reference frame. As a result, an orthogonal current signal is needed. Traditionally, this signal has been obtained from fixed time delays, digital filters or a Hilbert transformation. Nevertheless, these solutions present stability and transient drawbacks. Recently, the Fictive Axis Emulation (FAE) VOC has emerged as an alternative for the generation of the quadrature current signal. FAE requires detailed information of the grid current filter along with its transfer function for signal creation. When the transfer function is not accurate, the direct and quadrature current components present steady-state oscillations as the fictive two-phase system becomes unbalanced. Moreover, the digital implementation of the transfer function imposes an additional computing burden on the VOC. The PIFA VOC presented in this paper, takes advantage of the reference current to create the required orthogonal current, which effectively eliminates the need for the filter transfer function. Moreover, the fictive signal amplitude and phase do not change with a frequency drift, which results in an increased reliability. This yields a fast, linear and stable system that can be installed without fine tuning. To demonstrate the good performance of the PIFA VOC, simulation and experimental results are presented.

Key words: Current control, Fictive axis emulation, Grid filter, single phase inverter, Synchronous reference frame, Vector control

I. INTRODUCTION

Single-phase grid-tied Voltage Source Inverters (VSI) are used in a wide range of applications such as: renewable energy, uninterruptible power supplies, active power filters and power factor controllers [1]-[9]. These solutions, require a power converter capable of supplying an undistorted current while regulating the active and reactive power flow [9], [10]. To cope with these requirements, multilevel inverters, modified topologies, high order passive filters and different grid current control strategies have been explored [9]-[16]. Recently, different current controllers for single-phase controllers have been published, such as: hysteresis control, dead beat control, Proportional Integral (PI), proportional resonant current regulators, PLL compensators, fuzzy controllers, non-linear controllers and Voltage Oriented Control (VOC) [2], [16]-[25].

Active power filter applications based on model predictive control algorithms and a quasi z-source inverter were explored in [15]. This solution greatly reduces the cost of the system by reducing the voltage ripple on the DC link. Nevertheless, this arrangement requires careful tuning of the passive elements and control structure.

Non-linear controllers have recently received a lot of attention since they can operate without a Phase Locked Loop (PLL) and offer asymptotic stability and convergence. However, reactive power regulation and compatibility with advanced filters have not been covered in recent work [22], [25].

In most controller algorithms, the gain tuning becomes complex when filter topologies such as the LCL filter are used. In reference [12], a special direct current control tuning process is presented for three filter topologies. This process must be

Manuscript received Apr. 18, 2016; accepted Dec. 3, 2016
Recommended for publication by Associate Editor Hyung-Min Ryu.
†Corresponding Author: marjona@ieee.org
Tel: +52-871-7051331 ext 115, Fax: +52-871-7051326, Instituto Tecnológico de La Laguna
*Dept. of Electrical and Electronic Engineering, Instituto Tecnológico de La Laguna, Torreon, Mexico

repeated for every different filter topology and it may require extra effort to avoid oscillations when advanced filters such as the LLCL and $L(LCL)_2$ are considered [13].

Among the existing controllers, the VOC control algorithm stands out because of its low current THD, low sensitivity to frequency variations, compatibility with advanced modulation techniques and capacity for decoupled control of active and reactive power [23], [24], [26] and [27].

When dealing with a three-phase VOC controller, it is possible to transform the grid current into the synchronous reference frame. Thus, it is feasible to control the current using simple PI controllers with no steady-state error [24]. However, in a single-phase VSI, an orthogonal current signal is needed to emulate a two-phase system. This allows the transformation into the synchronous reference frame [21]. Different techniques have been employed for the creation of such signal. Some of these techniques include: fixed time delays, all-pass filters, Hilbert transformation and Fictive-Axis Emulation (FAE) [2], [5], [26]-[30].

Fixed time delayed signals disable the controller to cope with frequency variations as the phase shift will not correspond to 90 degrees. As a result, the quadrature system will no longer be valid. Furthermore, the presence of a quarter cycle delay in the β axis is detrimental for the system dynamic response since the synchronous frame response will be delayed by any perturbation [1], [2]. An alternative for generating such quadrature signal is the Hilbert transformation. However, this approach presents a high sensitivity to frequency fluctuations, and it has not gained industrial acceptance [2].

The FAE technique stands out as a recent and reliable development for generating the orthogonal current signal needed in reference frame transformations [1]. It is based on using the beta (V_β) component of the voltage command generated by the synchronous current regulator. Such signal is then used in conjunction with an artificial orthogonal voltage signal generated by a PLL. The aforementioned waveforms are used along with filter transfer functions, effectively creating a virtual quadrature axis. Still, detailed information on the grid voltage magnitude, filter parameters and its current transfer function are needed for effective axis emulation. Otherwise, double line frequency components appear in the control loops due to the imbalance between the real and imaginary currents. In other words, any deviation from the real values of the filter components and/or the grid voltage magnitude will produce an imaginary current that is neither orthogonal nor symmetric. Moreover, the digital implementation of complex transfer functions creates an added computational burden to the already computer intensive VOC algorithm.

In [23] a controller that employs an unbalanced reference frame is presented. The effects of the pulsating current are damped using a high bandwidth controller. This approach translates into different scenarios where different control structures are considered. However, this approach fails to present a single control structure that can be used in different applications without the need for further changes to the controller.

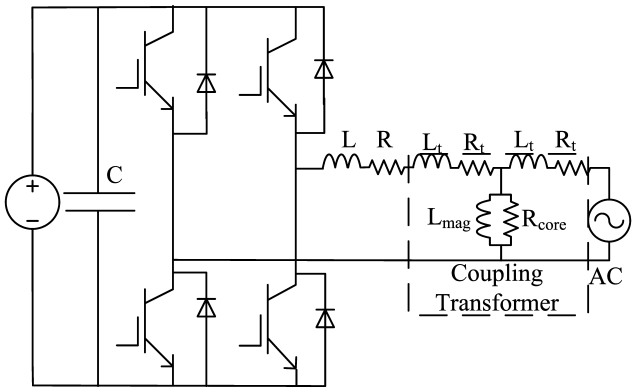

Fig. 1. Single-phase grid-tied inverter.

In this paper, a novel Parameter-Independent-Fictive Axis (PIFA) VOC algorithm is proposed to overcome dependence on filter parameters and controller tuning. This method is based on the assumption that a properly tuned controller keeps the grid current at its desired phase and magnitude values. Thereby, it is possible to use current reference values to generate the orthogonal current signal used in the reference frame transformation. Hence, a balanced, virtual axis is effectively created without the need for tight control loops or knowledge of the filter parameters. Furthermore, a precise voltage magnitude is not needed such as when dealing with a FAE VOC since the PLL is used solely for phase angle estimation. As a result, the generated quadrature current signal remains balanced regardless of frequency and parameter drifting. Hence, a reliable system that can be used under different grid impedances with little to no changes to the controller structure is attained. To demonstrate the functionality of the proposed approach, a single-phase PIFA VOC single-phase tied-grid inverter is developed. Simulation and experiments of the PIFA VOC and its comparison against the conventional FAE VOC are given.

II. GRID-TIED SINGLE-PHASE INVERTER

The layout of a single-phase grid-tied VSC is depicted in Fig. 1. The VSC is connected to an electric mains through an inductive current filter, although it may be substituted with other filter topologies such as the LC, LCL, LLCL and $L(LCL)_2$ filters.

The VOC controller is based on treating the grid as a virtual electrical machine. Accordingly, the filter inductance and resistance become analogous to stator parameters, while the grid voltages are treated as the voltages induced in the virtual electric machine. The grid voltage and current are assumed to be aligned along the α-axis. A fictitious quadrature axis, β, is created to transform the system into the

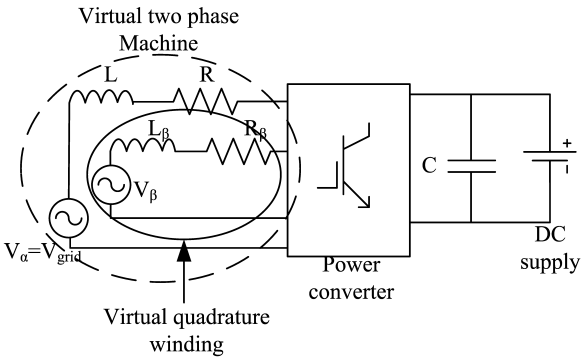

Fig. 2. Two-phase virtual machine.

synchronous reference frame.

The resultant virtual two-phase machine is illustrated in Fig. 2, and the voltage equation of such a system is given by (1).

$$V_{\alpha\beta} = RI_{\alpha\beta} + L\frac{dI_{\alpha\beta}}{dt} + V_{grid} \tag{1}$$

where R and L represent the line inductance and resistance, respectively, $V_{\alpha\beta}$ is the inverter voltage, $I_{\alpha\beta}$ is the grid current and V_{grid} is the grid-side voltage. If a decoupling network is used, Equ. (1) can be transformed into the synchronous reference frame, which leads to (2):

$$\begin{bmatrix} V_d \\ V_q \end{bmatrix} = L\begin{bmatrix} \frac{dI_d}{dt} \\ \frac{dI_q}{dt} \end{bmatrix} + \begin{bmatrix} R & 0 \\ 0 & R \end{bmatrix}\begin{bmatrix} I_d \\ I_q \end{bmatrix} + \begin{bmatrix} V_{gridd} \\ V_{gridq} \end{bmatrix} \tag{2}$$

where I_d and I_q are the direct and quadrature axis currents, respectively.

The current response of the system may be represented by the loop portrayed in Fig. 3 [1], [30]. Where I_d and I_q indicate the current components, K_p and T_i are the controller proportional and integral gains, and T_c is the sum of the sampling period and the inverter delay of the PWM modulation [32].

The following open-loop transfer function for I_d and I_q can be obtained (3):

$$\frac{I(s)}{I^*(s)} = \frac{K_p(T_i s+1)}{T_i s(sT_c+1)(sL+R)} \tag{3}$$

This function presents a dominant pole (Ls+R). Therefore, the current loop tuning may be achieved by considering a second order element [1], [27].

III. Parameter-independent Fictive-axis Current Control

The FAE algorithm is based on the application of the difference between the V_β command and a PLL synthesized quadrature voltage waveform ($V_{mag}\sin\theta$) of the current transfer function of the grid-filter. The block diagram is depicted in Fig. 4, where V_{mag} is the estimated grid voltage, and θ is the PLL estimated phase angle.

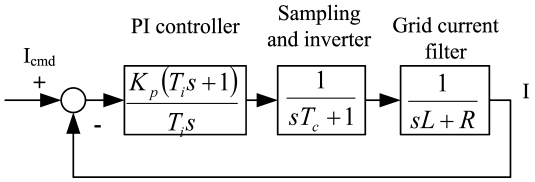

Fig. 3. System current loop.

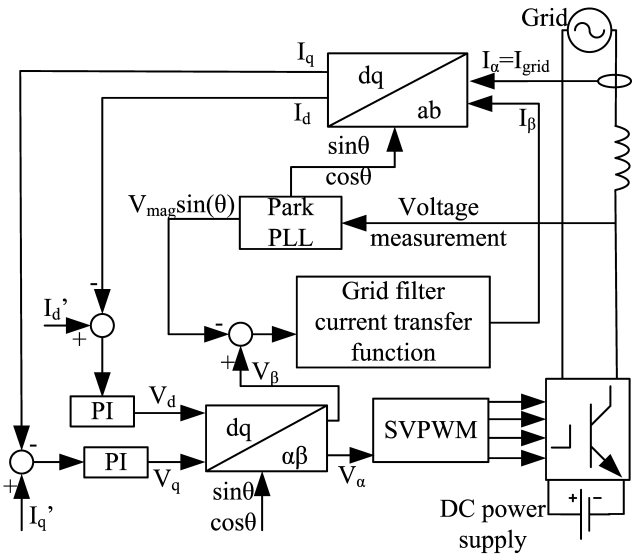

Fig. 4. Fictive axis single-phase vector control.

Consequently, a fictitious orthogonal current is created and both the grid current and its orthogonal counterpart are then used to drive the reference frame transformations needed for the use of a synchronous current regulator. Thus, a system with a fast dynamic response is achieved at the cost of becoming dependent on the grid parameters and voltage magnitude estimation. On the other hand, the proposed PIFA alternative eliminates such dependence by generating orthogonal current signals using the I_d' and I_q' references to create the β-axis. Thus, I_β is obtained by using (4):

$$I_\beta = I_d'\sin\theta + I_q'\cos\theta \tag{4}$$

The block diagram for the proposed algorithm is shown in Fig. 5. The I_β generation is based on the assumption that a properly tuned current regulator will keep the current values at the same level of the references. Therefore, an orthogonal current is effectively created for the reference frame transformation without knowledge of filter parameters or the value of the grid voltage magnitude.

Under this approach, the grid voltage measurement is merely used to drive a PLL which generates the sin(θ) and cos(θ) signals used during reference frame transformations.

On the synchronous reference frame, the desired inverter voltages are attained from current control loops. Once the direct and quadrature voltage commands (V_d and V_q) have been obtained, they are then used to synthesize V_α.

This signal drives the modulation algorithm that creates the firing signals for the VSI. With this approach, the V_β signal created from the current loop is not needed.

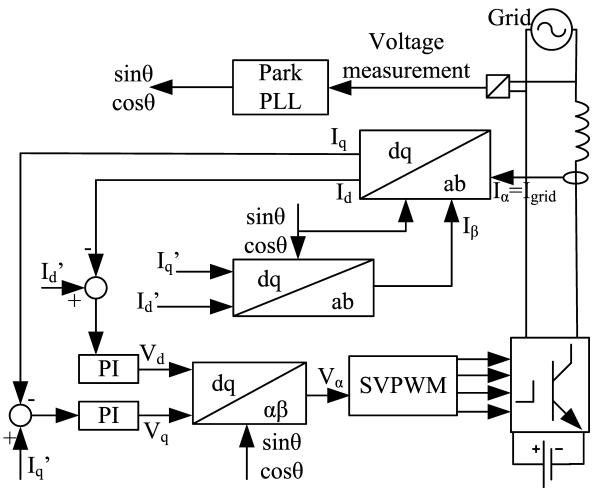

Fig. 5. Parameter-independent fictive-axis vector control.

TABLE I
SYSTEM PARAMETERS

Symbol	QUANTITY	Magnitude
C	DC bus capacitor	2700 uF
L	Filter inductance	9.02 mH
R	Filter resistance	1.4 Ω
N	Transformer ratio	4 (120V/30V)
V_{cc}	DC bus voltage	70 V
F	Grid frequency	60 Hz
F_c	Commutation frequency	6 kHz
F_s	Sampling rate	6 kHz
K_p	Proportional Gain	20.954
K_i	Integral Gain	20954

IV. SIMULATION AND EXPERIMENTAL EVALUATION

The proposed system is evaluated against the FAE VOC. The steady-state and dynamic responses of the PIFA VOC algorithm are evaluated by simulations and experiments. The system parameters used in the simulations are given in Table I.

A. Simulation Study

The PIFA and FAE VOC control strategies were evaluated using MATLAB/Simulink.

The current control loop was tuned using the modulus optimum algorithm. The simulation comparison was carried out considering a 10% deviation in the grid voltage magnitude and a 10% deviation in the filter inductance. The dynamic responses of both control algorithms were evaluated with an instantaneous step change at 0.5 ms in the current commands from I_d=0A and I_q=-3A to I_d=6A. The I_d and I_q current components are depicted in Fig. 6.

Both systems presented a fast transient response (<3 ms). Nevertheless, the presence of magnetization reactance and equivalent core resistance represent a deviation from the grid impedance parameters used in the fictive axis emulation.

Thus, steady-state oscillations appear in the I_{dq} current components. The amplitude for such oscillations increases from 160 mA to 211 mA when a 10% deviation is considered in the grid voltage. On the other hand, this variation presented no effect on the PIFA-VOC performance. The grid current waveforms for such test are shown in Fig. 7. It can be seen that the proposed PIFA VOC produces an instantaneous change on the I_β current component, when compared with the

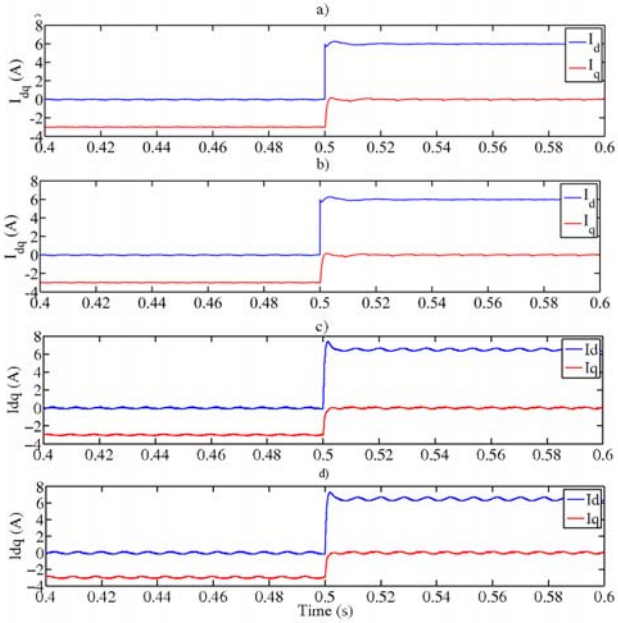

Fig. 6. I_q current transition from -3A to 0 A, and from 0A to 6.5 A on I_d. (a) PIFA current controller. (b) PIFA current controller with 10% deviation from grid voltage measurement. (c) FAE current controller. (d) FAE current controller with 10% deviation from grid voltage measurement.

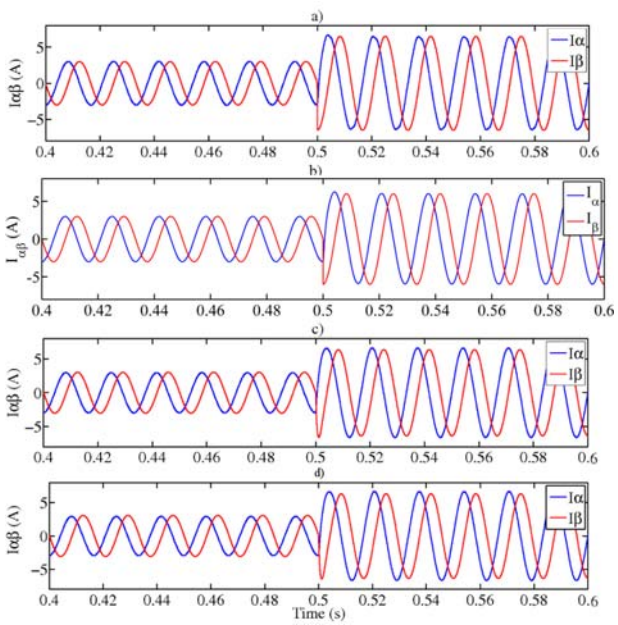

Fig. 7. Response of $I_{\alpha\beta}$ currents during a reference perturbation. (a) PIFA current controller. (b) PIFA current controller with 10% deviation from grid voltage measurement. (c) FAE current controller. (d) FAE current controller with 10% deviation from grid voltage measurement.

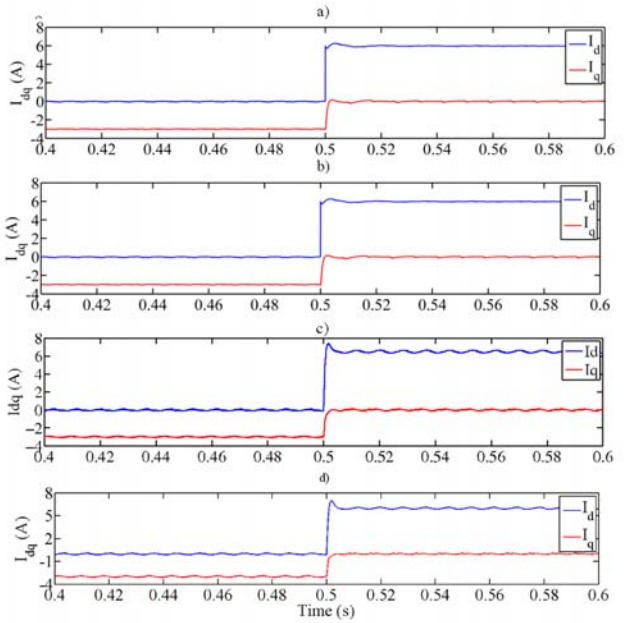

Fig. 8. Response of I_{dq} currents during a reference perturbation. (a) PIFA current controller. (b) PIFA current controller with 10% deviation from filter inductance. (c) FAE current controller. (d) FAE current controller with 10% deviation filter inductance.

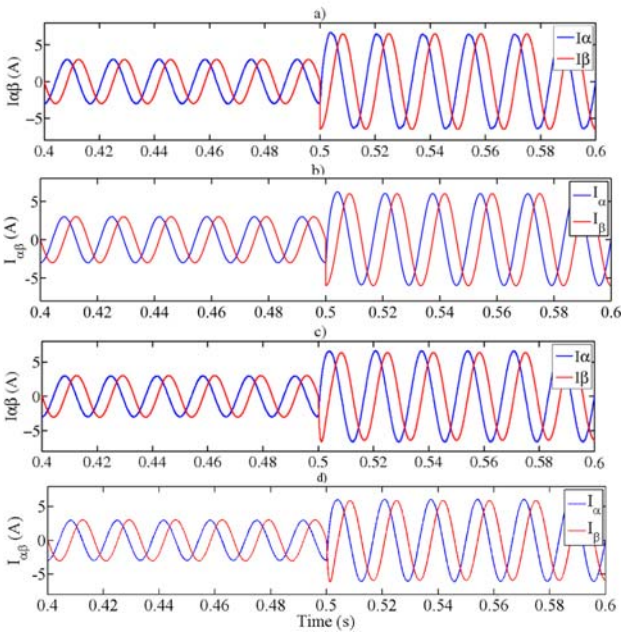

Fig. 9. Response of I_α and I_β during reference perturbation. (a) PIFA current controller. (b) PIFA current controller with 10% deviation from filter inductance. (c) FAE current controller. (d) FAE current controller with 10% deviation filter inductance.

FAE current I_β at 2.6 ms. This difference is produced by the dynamic response of the β axis fictive current filter. Nevertheless, this difference is so small that it has no detrimental effect on the response of the PIFA-VOC system.

A comparison considering a 10% deviation on L is portrayed in Figs. 8 and 9. Again, the PIFA-VOC controller shows no steady-state oscillations while the FAE-VOC

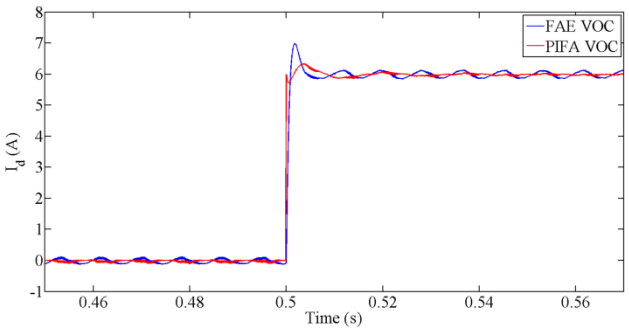

Fig. 10. Current (I_d) dynamic response with a 10% inductance variation.

TABLE II
TUNED SYSTEM PARAMETERS

Eigenvalue	DAMPING	Frequency (Hz)
-2.33E03	1.0	370.8310
-1920 + 1520j	0.784	389.9296
-1920 - 1520j	0.784	389.9296

presented 280mA oscillations when the inductance deviation is considered.

A detailed plot of the current dynamic response when the inductance is deviated is illustrated in Fig. 10. Even though L is a part of the current decoupling network, the effect of the variation is more evident in the FAE system where a larger overshoot is observed (16% when compared with the 5% of the PIFA response). This response is related to the detrimental effect oscillations have on PI controllers.

Since the difference of the proposed system relies on fictive axis generation, the current transfer function remains the same. These systems present three poles: a real one and a couple of complex ones (Table II). The damping associated with the complex roots corresponds to an under damped system with a natural frequency of 389.9 Hz. This observation corresponds to the impulse observed in the current response shown in Fig. 6.

B. Experimental Evaluation

In order to demonstrate its validity, the PIFA current controller was experimentally evaluated. The test system is implemented in a dsPIC33FJ128MU802 DSC. The grid voltage and current waveforms were measured using the LV-25P and CSLA2CD Hall effect sensors, respectively. The DC bus voltage was generated using a DC source along with the DC bus voltage capacitors listed in Table I. The rest of the system parameters are the same as those used in the simulation study previously described. The behavior of the PIFA VOC current controller is evaluated in both steady-state and dynamic operation.

The current waveform along with the power delivered to the grid during steady-state operation (I_d=6A) can be observed in Fig. 11. As can be clearly seen, a sinusoidal

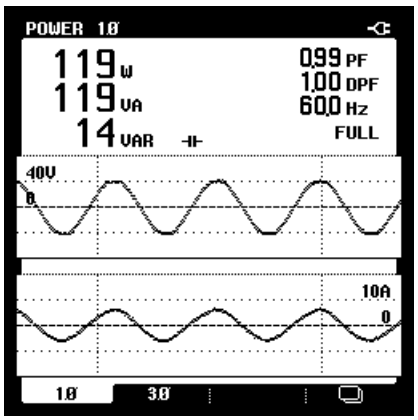

Fig. 11. Experimental PIFA VOC power profile along voltage and current waveforms.

Fig. 12. Experimental PIFA VOC current harmonic profile.

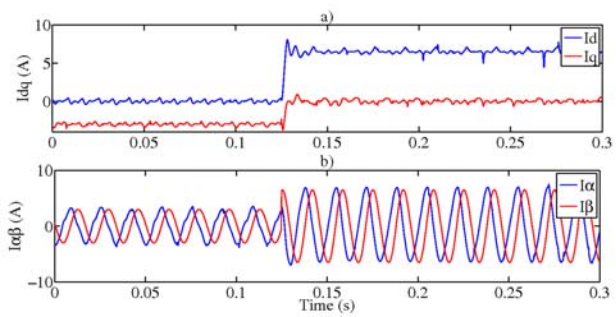

Fig. 13. Experimental PIFA current during an instantaneous reference change a) I_d and I_q components, b) I_α and I_β currents.

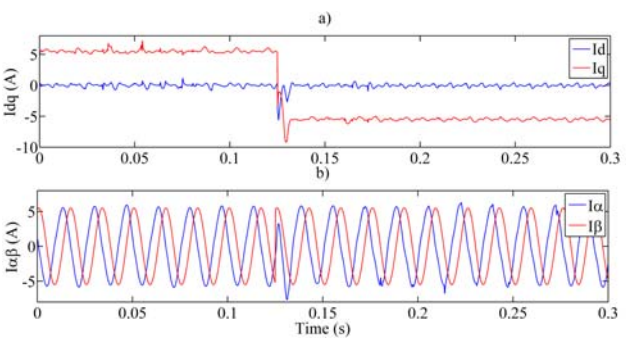

Fig. 14. Experimental PIFA current during change from delivering inductive reactive power to capacitive reactive power a) I_d and I_q components b) I_α and I_β currents.

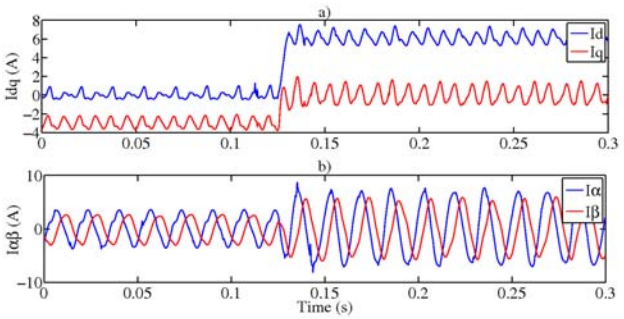

Fig. 15. Experimental FAE current during an instantaneous reference change a) I_d and I_q components b) I_α and I_β currents.

current waveform is delivered to the grid with practically a unitary power factor. The THD and Fourier spectrum of the current are portrayed in Fig. 12, where a near sinusoidal waveform (THD less than 2.5%) may be observed. These low THD values correspond with the grid current waveforms that are observed in both the simulation and experimental results when the I_d current component is properly regulated.

The dynamic response of the PIFA system was evaluated using the same perturbation of the current reference used during the simulation analysis. The current waveforms were stored in the controller memory and then retrieved using the Data Monitor Control Interface embedded in MPLAB IDE [33]. Afterwards, the experimental current data was plotted using Matlab.

The dynamic response of the experimental I_{dq} and $I_{\alpha\beta}$ current components under the PIFA VOC is portrayed in Fig. 13, where the current reference is changed from -3 A to 0 A on I_q and from 0 A to 6.5 A on I_d at 0.125 s. The system retained a fast dynamic response because the orthogonal current component presents an instantaneous response, while the grid current reaches the desired magnitude and phase values in less than 3 ms.

Additionally, the system response when the converter passes from delivering inductive reactive power to capacitive reactive power is portrayed in Fig. 14. The transition is done from 5 A to -5 A on the quadrature axis at t=0.125 s. During the transition, the system exhibits a fast and stable response even during a phase change of 180 degrees. During these tests the system portrayed a stable sinusoidal current waveform without overcurrent spikes or oscillations during the changes from one operation state to the other.

The FAE VOC controller was also implemented and its experimental response is portrayed in Fig. 15. A fast transient response was attained with a similar behavior in the αβ axes when compared with the PIFA-VOC.

Nevertheless, as predicted by the simulation analysis, a steady state oscillation on the I_{dq} current components may be observed. Such oscillations are attributed to the presence of the transformer magnetization reactance which represent a discrepancy between the overall estimated current transfer function and the real one. These results reinforce the

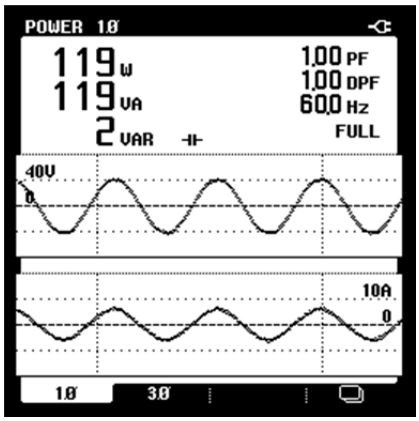

Fig. 16. Experimental FAE VOC power profile along voltage and current waveforms.

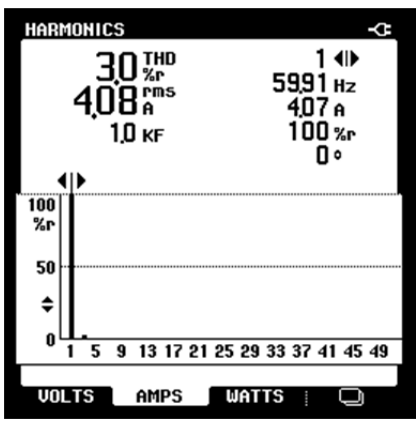

Fig. 17. Experimental FAE VOC current harmonic profile.

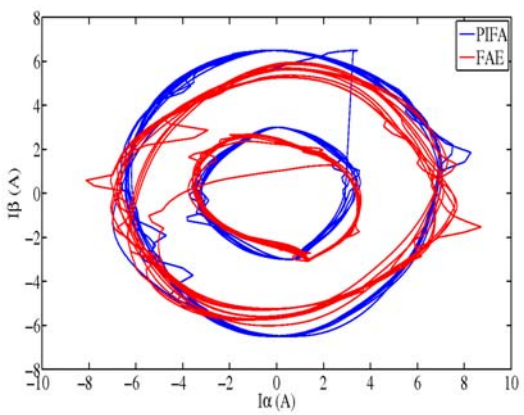

Fig. 18. Experimental AC current trajectories during an instantaneous reference change.

sensitivity of the FAE-VOC controller to overall grid/filter impedance. As a result, I_α and I_β become unbalanced, which affects the overall system performance.

The FAE stationary performance can be observed in Figs. 16 and 17 (I_d=6A), where a unit power factor and a 3% THD are observed. The increase in the current THD with respect to the PIFA VOC system is attributed to the steady state oscillations on the I_{dq} components that prevent the PI regulators from reaching a final value.

The aforementioned is confirmed by the experimental AC current trajectories of both the PIFA and FAE (Fig. 18). As can be observed, the PIFA current controller presents a more symmetric pattern since the amplitude and phase angle of the I_β current controller are not related to the estimated grid parameters or to the accurate estimation of the grid voltage with the PLL. Consequently, the orthogonal current remains at its desired value independently of the existent impedance between the VSI and the grid, which produces a true orthogonal system.

V. Conclusions

The design and implementation of a novel Parameter Independent Fictive Axis (PIFA) approach for the VOC algorithm used in single-phase inverters have been presented. The quadrature current signal needed for reference frame transformations is obtained from current reference commands. The proposed algorithm improves the system dynamic response when compared to fixed-delay structures, and it is independent of the grid frequency. Moreover, the proposed PIFA presents an improved flexibility when compared to the conventional FAE VOC since it does not require knowledge of the filter transfer function or its parameters. Additionally, this system is not dependent on the estimation of the voltage accuracy since the PLL functionality is limited to phase estimation.

The proposed PIFA algorithm was evaluated in simulation and experimental analysis and it was compared against the conventional FAE VOC. The PIFA-VOC system presents excellent features such as: good dynamic response (<3 ms), non-pulsating current components, zero steady-state error, and sinusoidal current waveform (THD<2.5%).

These experimental results are similar to those obtained from the FAE system. Nevertheless, the main difference resides on the absence of I_{dq} current oscillations, the improved THD (3.1% for the FAE system), and the elimination of grid transfer function estimation. Thus, a lower computational time can be attained. It is demonstrated that it is feasible to implement a reliable parameter independent VOC single-phase grid-tied inverter without detailed knowledge of the impedance between the VSI and the grid.

References

[1] B. Bahrani, A. Rufer, S. Kenzelmann, and L. A. C. Lopes, "Vector control of single-phase voltage-source converter based on fictive-axis emulation," *IEEE Trans. Ind. Appl.*, Vol. 47, No. 2, pp. 831-840, Apr. 2011.

[2] M. Monfared, and S. Golestan, "Control strategies for single-phase grid integration of small-scale renewable energy sources: A review," *Renewable and Sustainable Energy Reviews*, Vol. 16, No. 7, pp. 4982-4993, Sep. 2012.

[3] E. Puresmaeil, O. Gomis-Bellmunt, D. Montesinos-Miracle, and J. Bergas-Jane "Multilevel converters control for renewable energy integration to the power grid," *Energy*, Vol. 36, No. 2, pp. 950-963, Feb. 2011.

[4] C. G. C. Branco, C. M. T. Cruz, R. P. Torrico-Bascope, and F. L. M. Antunes, "A nonisolated single-phase UPS topology with 110-V/220-V input–output voltage ratings," *IEEE Trans. Ind. Electron.*, Vol. 55, No.8, pp. 2974-2983, Aug. 2008.

[5] K. Bong-Hwan, C. Jin-Ha, and K. Tae-Won Kim, "Improved single-phase line-interactive UPS," *IEEE Trans. Ind. Electron.*, Vol.48, No. 4, pp. 804-811, Aug. 2001.

[6] F.A. Ramirez and M. A. Arjona, "Development of a grid-connected wind generation system with a modified PLL structure," *IEEE Trans. Sustain. Energy*, Vol.3, No.3, pp. 474-481, Jul. 2012.

[7] H. Khan, S. Dasouki, V. Sreeram, H. H. C. Iu, and Y. Mishra, "Universal active and reactive power control of electronically interfaced distributed generation sources in virtual power plants operating in grid connected and islanding modes," *IET Generation, Transmission & Distribution*, Vol. 7, No. 8, pp. 885-897, Aug. 2013.

[8] W. R. Nogueira Santos, E. R. Cabral da Silva, C. Brandao Jacobina, E. de Moura Fernandes, A. Cunha Oliveira, R. Rocha Matias, D. Franca Guedes Filho, O. M. Almeida, and P. Marinho Santos, "The transformerless single-phase universal active power filter for harmonic and reactive power compensation," *IEEE Trans. Power Electron.*, Vol. 29, No. 7, pp. 3563-3572, Jul. 2014.

[9] R. A. Mastromauro, M. Liserre, T. Kerekes, and A. Dell'Aquila, "A single-phase voltage-controlled grid-connected photovoltaic system with power quality conditioner functionality," *IEEE Trans. Ind. Electron.*, Vol. 56, No. 11, pp. 4436-4444, Nov. 2009.

[10] W. Tsai-Fu, S. Kun-Han, K. Chia-Ling, and C. Chih-Hao, "Predictive current controlled 5-kW single-phase bidirectional inverter with wide inductance variation for DC-microgrid applications," *IEEE Trans. Power Electron.*, Vol. 25, No. 12, pp. 3076-3084, Dec. 2010.

[11] X. Shungang, W. Jinping, and X. Jianping, "A current decoupling parallel control strategy of single-phase inverter with voltage and current dual closed-loop feedback," *IEEE Trans. Ind. Electron.*, Vol. 60, No. 4, pp. 1306-1313, Apr. 2013.

[12] F. A. Ramirez and M. A. Arjona, "An improved SVPWM control of voltage imbalance in capacitors of a single-phase multilevel inverter," *Journal of Power Electronics*, Vol. 15, No. 5, pp. 1235-1243, Sep. 2015.

[13] A. Anzalchi, M. Moghaddami, A. Moghadasi, A. Sarwat, and A. Rathore, "A new topology of higher order power filter for single-phase grid-tied voltage source inverters," *IEEE Trans. Ind. Electron.*, Vol. 63, No. 12, pp. 7511-7522, Jul. 2016.

[14] S. Li, X. Fu, M. Ramezani, Y. Sun, and H. Won, "A novel direct-current vector control technique for single-phase inverter with L, LC and LCL filters," *Electric Power Systems Research*, Vol. 125, pp. 235-244, Aug. 2015.

[15] Y. Liu, B. Ge, H. Abu-Rub, H. Sun, F. Z. Peng, and Y. Xue, "Model predictive direct power control for active power decoupled single-phase quasi-z -source inverter," *IEEE Trans. Ind. Inform.*, Vol. 12, No. 4, pp. 1550-1559, Aug. 2016.

[16] A. Radhika and A. Shunmugalatha, "A novel photovoltaic power harvesting system using a transformerless h6 single-phase inverter with improved grid current quality," *Journal of Power Electronics*, Vol. 16, No. 2, pp. 654-665, Mar. 2016.

[17] P. A. Dahono, "New hysteresis current controller for single-phase full-bridge inverters," *IET Power Electron.*, Vol. 2, No. 5, pp. 585-594, Sep. 2009.

[18] R. Teodorescu, F. Blaabjerg, M. Liserre, and P. C. Loh, "Proportional-resonant controllers and filters for grid-connected voltage-source converters," in *IEE Proc. Electric Power Applications*, Vol. 153, No. 5, pp. 750-762, 2006.

[19] C. Bao, X. Ruan, X. Wang, W. Li, D. Pan, and K. Weng, "Step-by-step controller design for LCL-type grid-connected inverter with capacitor–current-feedback active-damping," *IEEE Trans. Power Electron.*, Vol. 29, No. 3, pp. 1239-1253, Mar. 2014.

[20] S. K. Hung, H. B. Shin, and H.W. Lee, "Precision control of single-phase PWM inverter using PLL compensation," in *IEE Proc. Electric Power Applications*, Vol. 152, No. 2, pp. 429-436, 2005.

[21] K. A. Run and K. Selvajyothi, "Observer based current controlled single phase grid connected inverter," in *Int. Conf. on Design and manufacturing in Procedia Engineering,* Vol. 64, pp. 367-376, 2013.

[22] G. C. Konstantopoulos, and Q. C. Zhong, "Nonlinear control of single-phase PWM rectifiers with inherent current-limiting capability," *IEEE Access*, Vol. 4, pp. 3578-3590, Jun. 2016.

[23] S. Somkun and V. Chunkag, "Unified unbalanced synchronous reference frame current control for single-phase grid-connected voltage-source converters," *IEEE Trans. Ind. Electron.*, Vol. 63, No. 9, pp. 5425-5436, Sep. 2016.

[24] B. Saritha and P.A. Jankiraman, "Observer based current control of single-phase inverter in DQ rotating frame," in *International Conference on Power Electronics, Drives and Energy Systems, PEDES*, pp.1-5, 2006.

[25] G. C. Konstantopoulos, Q. C. Zhong, and W. L. Ming, "PLL-less nonlinear current-limiting controller for single-phase grid-tied inverters: design, stability analysis, and operation under grid faults," *IEEE Trans. Ind. Electron.*, Vol. 63, No. 9, pp. 5582-5591, Sep. 2016.

[26] M. P. Kazmierkowski and L. Malesani, "Current control techniques for three-phase voltage-source PWM converters: A survey," *IEEE Trans. Ind. Electron.*, Vol. 45, No. 5, pp. 691-703, Oct. 1998.

[27] B. Crowhurst, E.F. El-Saadany, L. El Chaar, and L.A. Lamont, "Single-phase grid-tie inverter control using DQ transform for active and reactive load power compensation," in *IEEE International Conference on Power and Energy*, pp. 489-494, 2010.

[28] L. Padmavathi, and P. A. Janakiraman, "Self-tuned feed-forward compensation for harmonic reduction in single-phase low-voltage inverters," *IEEE Trans. Ind. Electron.*, Vol. 58, No. 10, pp. 4753-4762, Oct. 2011.

[29] M. Saitou and T. Shimizu, "Generalized theory of instantaneous active and reactive powers in single-phase circuits based on Hilbert transform," in *Power Electronics Specialists Conference*, Vol. 3, pp. 1419-1424, 2002.

[30] M. Saitou, N. Matsui, and T. Shimizu, "A control strategy of single-phase active filter using a novel d-q transformation," in *Industry Applications Conference*, Vol. 2, pp.1222-1227, 2003.

[31] S. Somkun and V. Chunkag, "Unified unbalanced synchronous reference frame current control for single-phase grid-connected voltage-source converters,"

IEEE Trans. Ind. Electron., Vol. 63, No. 9, pp. 5425-5436, Sep. 2016.
[32] V. Blasko and V. Kaura, "A new mathematical model and control of a three-phase AC-DC voltage source converter," *IEEE Trans. Power Electron.*, Vol. 12, No. 1, pp. 116-123, Jan. 1997.
[33] M. Jasinski, "Direct power and torque control of AC/DC/AC converter-fed induction motor drives," PhD. Dissertation, Warsaw University of Technology, Poland 2005.
[34] Microchip, *Real Time Data Monitor User's Guide*, DS70567A, Microchip technology Inc., 2008.

Fernando Arturo Ramírez received his B.S. degree in Electronic Engineering; and his M.S. and PhD. degrees in Electrical Engineering from the La Laguna Institute of Technology, Coahuila, México, in 2010 and 2015 respectively. He is presently working as a Professor of Power Electronics at the La Laguna Institute of Technology. His current research interests include power converters, motor control, and renewable energy.

Marco A. Arjona received his B.S. degree from the Durango Institute of Technology, Durango, Mexico, in 1988; his M.S. degree from the La Laguna Institute of Technology, Coahuila, México, in 1990; and his Ph.D. degree from the Imperial College, London, ENG, UK, in 1996, all in Electrical Engineering. He was with the Simulation Department of the Mexican Electrical Research Institute from 1991 to 1999. He is presently working as a Professor of Electrical Machines at La Laguna Institute of Technology. His current research interests include the design, analysis, and control of electrical machines and renewable energy.

Concepcion Hernández received her B.S. degree in Computer Science from the Instituto Tecnológico de Estudios Superiores de Monterrey, Monterrey, México, in 1990; her M.S. degree in Foundations of Advanced Information Technology from Imperial College, London, ENG, UK, in 1995; and her Ph.D. degree in Electrical Engineering from the Instituto Tecnológico de la Laguna, Torreón, México, in 2007. She was with the Simulation Department, Instituto de Investigaciones Eléctricas from 1991 to 2000. She is presently working at the Instituto Tecnológico de la Laguna, Torreón, México. Her current research interests include artificial intelligence and global optimization algorithms applied to electrical machines.